


RESEARCH

Open Access



# S1PR3 inhibition impairs cell cycle checkpoint via the AKT/WEE1 pathway in oral squamous cell carcinoma

Xinxia Zhou<sup>1</sup>, Jinghao Liu<sup>1</sup>, Xu Chen<sup>1</sup>, Xinyu Zhou<sup>3</sup>, Beihui Xu<sup>1</sup>, Guifang Gan<sup>1\*</sup> and Fuxiang Chen<sup>1,2\*</sup> 

## Abstract

**Background** Sphingosine-1-phosphate receptor 3 (S1PR3) has been implicated in promoting tumor progression in various cancers. However, the role and molecular mechanisms of S1PR3 in oral squamous cell carcinoma (OSCC) remain poorly understood. The aims of this study were to investigate the function of S1PR3 in OSCC progression and its potential as a therapeutic target.

**Method** The expression of S1PR3 was determined through qPCR, Western blotting analysis, immunohistochemistry (IHC), and the TCGA database. The correlation between *S1PR3* expression and clinical prognosis was analyzed using the TCGA database and IHC. The effects of S1PR3 on OSCC cell proliferation and cell cycle were investigated through CCK-8 assay, colony formation assay, EdU incorporation assay, cell cycle analysis, and a xenograft mouse model. The potential mechanisms through which *S1PR3* affects the OSCC cell cycle were explored using RNA-seq and a cell cycle array. The effects of combining S1PR3 antagonist with cisplatin on OSCC cell growth were examined through CCK-8 and EdU incorporation assays.

**Results** *S1PR3* was overexpressed in OSCC and the upregulation of *S1PR3* in OSCC was correlated with unfavorable clinicopathological characteristics and adverse prognosis. Targeting *S1PR3* reduced AKT phosphorylation, which led to a downregulation of WEE1, a kinase involved in cell cycle regulation. This downregulation resulted in reducing CDC2 phosphorylation, disrupting the G2/M cell cycle checkpoint and inhibiting OSCC cell proliferation. Furthermore, the combination of S1PR3 antagonist exhibited synergistic inhibitory effects on OSCC cell growth when combined with cisplatin.

**Conclusions** These findings reveal a critical role for S1PR3 in regulating OSCC cell cycle via the AKT/WEE1/CDC2 pathway, thus offering a basis for developing treatment strategies for OSCC patients.

**Keywords** Oral squamous cell carcinoma, Sphingosine-1-phosphate receptor 3, AKT signaling pathway, WEE1, Cell cycle

\*Correspondence:

Guifang Gan  
agan1992@126.com  
Fuxiang Chen  
chenfx@sjtu.edu.cn

Full list of author information is available at the end of the article



© The Author(s) 2025. **Open Access** This article is licensed under a Creative Commons Attribution-NonCommercial-NoDerivatives 4.0 International License, which permits any non-commercial use, sharing, distribution and reproduction in any medium or format, as long as you give appropriate credit to the original author(s) and the source, provide a link to the Creative Commons licence, and indicate if you modified the licensed material. You do not have permission under this licence to share adapted material derived from this article or parts of it. The images or other third party material in this article are included in the article's Creative Commons licence, unless indicated otherwise in a credit line to the material. If material is not included in the article's Creative Commons licence and your intended use is not permitted by statutory regulation or exceeds the permitted use, you will need to obtain permission directly from the copyright holder. To view a copy of this licence, visit <http://creativecommons.org/licenses/by-nc-nd/4.0/>.

## Introduction

Head and neck cancers rank as the sixth most prevalent cancer globally, with oral squamous cell carcinoma (OSCC) constituting approximately 90% of all cases [1, 2]. According to GLOBOCAN 2020 statistics, an estimated 377 713 new cases and 177 757 deaths due to oral cancer are reported annually [3]. Current OSCC treatments include primarily surgery, radiotherapy and chemotherapy, which possess limited efficacy, with 25–50% of OSCC patients experiencing recurrence [4]. In addition, radiotherapy and chemotherapy are frequently associated with adverse effects, including dermatitis, osteoradionecrosis and nephrotoxicity, thus significantly impairing patients' quality of life [5, 6]. Moreover, the tendency of OSCC to metastasize and recur combined with low cure rates and high mortality rates constitute substantial challenges for patients and their families [7]. Therefore, it is imperative to advance research into the molecular basis of OSCC development to identify novel treatment targets.

As members of the G-protein-coupled receptor (GPCR) family, sphingosine-1-phosphate receptors (S1PRs) are categorized into five distinct subtypes, i.e., S1PR1–S1PR5. Therapies targeting these receptors are widely recognized as promising strategies, given their prior use in treating immune diseases such as ulcerative colitis and multiple sclerosis [8]. Emerging evidence suggests that dysregulated S1PR expression is pivotal in the progression of multiple cancers [9]. Therefore, it can be hypothesized that the *S1PR* family may constitute potential targets for preventing OSCC progression. More evidence suggests that S1PR3 contributes to the progression of multiple cancers, including osteosarcoma, gastric cancer and nasopharyngeal carcinoma, thus influencing key biological processes within tumor cells such as proliferation, migration, apoptosis and invasion [10]. However, the specific biological mechanisms by which S1PR3 contributes to OSCC remain to be clarified.

In the present study, we demonstrated that *S1PR3* was overexpressed in OSCC and correlated with advanced clinical stages and adverse prognosis in OSCC patients, suggesting that *S1PR3* may act as a pro-tumorigenic factor in OSCC development. Notably, targeting *S1PR3* significantly reduced OSCC cell growth both in vitro and in vivo. Further mechanistic investigations demonstrated that targeting *S1PR3* inhibited WEE1 expression via the AKT signaling pathway, which subsequently reduced CDC2 phosphorylation and disrupted the G2/M cell cycle checkpoint. Moreover, our results showed that the S1PR3 antagonist CAY10444 exhibited synergistic inhibition of OSCC cell growth when combined with cisplatin. Therefore, the S1PR3/AKT/WEE1 signaling pathway

constitutes a promising potential target for the treatment of OSCC.

## Materials and methods

### Cell lines

Human immortalized keratinocyte cell line (HaCat) and HNSCC cell lines WSU-HN4, WSU-HN6, CAL27 and WSU-HN30 were obtained from Department of Oral Oncology, Ninth People's Hospital, Shanghai Jiao Tong University School of Medicine, China. Cells were maintained at 37 °C in a humidified chamber with 5% CO<sub>2</sub>, using Dulbecco's Modified Eagle's Medium (DMEM; Gibco, NY, USA) containing 10% fetal bovine serum and 1% penicillin–streptomycin.

### Reagents and antibodies

The S1PR3 antagonist CAY10444 (Selleckchem, TX, USA) and the AKT agonist SC79 (Selleckchem) were prepared and stored following the manufacturer's guidelines. S1PR3 and S1PR4 antibodies were obtained from Abcam PLC (Cambridge, UK). S1PR1, S1PR2 and S1PR5 antibodies were obtained from ProteinTech Group, Inc. (IL, USA). AKT, p-AKT, WEE1, CDC2, p-CDC2 and GAPDH antibodies were obtained from Cell Signaling Technology, Inc. (MA, USA).

### Bioinformatics analysis

Transcriptomic data of HNSCC patients were retrieved from TCGA. Based on the median expression level, patients were classified into *S1PR3* high- and low-expression groups. The correlation between *S1PR3* expression and overall survival (OS), disease-specific survival (DSS), as well as progression-free interval (PFI) was evaluated using GraphPad Prism 8.0.2 software. Hazard ratios (HR) and 95% confidence intervals (CI) were calculated.

### Tissue specimens and tissue microarray

Tumor tissues and adjacent tissues from OSCC patients were collected from the Department of Oral Pathology, Ninth People's Hospital, Shanghai Jiao Tong University School of Medicine, China. A tissue microarray (TMA) was constructed by Taize Biotechnology Co., Ltd. (Guangzhou, China) using samples from OSCC patients.

### Xenograft mouse model

Four-week-old male BALB/c nude mice were sourced from the Animal Experiment Center of the Ninth People's Hospital, Shanghai Jiao Tong University School of Medicine, China and reared in the same facility. 2 × 10<sup>7</sup> *S1PR3* knockdown CAL27 cells, along with control cells, were subcutaneously injected in mice's inguinal region. Once xenograft tumors became palpable, mice body weight and tumor volume (tumor volume = tumor

width<sup>2</sup> × tumor length/2) were recorded every five days. After 20 days, the mice were euthanized and the excised xenograft tumors were weighed and captured in images.

For chronic drug administration,  $2 \times 10^7$  *S1PR3* knock-down CAL27 cells, along with control cells, were subcutaneously injected in mice's inguinal region. Once xenograft tumors reached an appropriate size, the mice were divided into control and treatment groups using random assignment (5/group), which were intraperitoneal injected with SC79 (20 mg/kg) or dimethyl sulfoxide. Drugs were administered every three days and mice body weight and tumor volume were recorded. After 12 days, the mice were euthanized and the excised xenograft tumors were weighed and captured in images. Excised tumor sections were fixed in 4% paraformaldehyde in preparation for immunohistochemical (IHC) assays. See the section on IHC assays in Materials and Methods for details.

#### IHC assays

IHC assays were performed to evaluate *S1PR3* expression in clinical samples and protein levels of *S1PR3*, p-AKT, *WEE1* and *Ki67* in xenograft tumors from nude mice. Paraffin-embedded OSCC sections were dewaxed, rehydrated and subjected to antigen retrieval in citrate buffer (pH 6.0) for 15 min. Sections were treated with 3% H<sub>2</sub>O<sub>2</sub> for 10 min to block endogenous peroxidase activity. Following overnight incubation with primary antibodies at 4 °C, sections were incubated with secondary antibodies for 1 h at room temperature. Visualization was achieved using DAB, followed by hematoxylin counterstaining. Stained sections were analyzed under a light microscope (Olympus, Tokyo, Japan).

#### RNA extraction, qPCR validation and PCR array

Total RNA was extracted with TRIzol reagent (Invitrogen Corporation, CA, USA) and then converted into cDNA with a reverse transcription kit (TaKaRa Biotechnology Co., Ltd., Kyoto, Japan). cDNA amplification was carried out via qPCR with the SYBR Premix Ex Taq II kit (TaKaRa) in triplicate in a 96-well plate. qPCR processes were conducted on an Applied Biosystems™ 7500 Real-Time PCR system (Life Technologies, NY, USA) employing primers specified in Supplementary Table 1 and in accordance with the manufacturer's protocol. The  $2^{-\Delta\Delta C_t}$  method was used to measure mRNA levels, with *β-actin* serving as the reference gene. Cell cycle-related genes showing significant differential expression after CAY10444 treatment were identified using a human cell cycle PCR array kit (Wcgene Biotech, Shanghai, China).

#### Gene knockdown experiments

Short-hairpin RNAs (shRNAs) (Genomeditech, Shanghai, China) were employed to silence *S1PR3* in OSCC cells. Supplementary Table 2 contains the shRNA sequences designed to target *S1PR3*. Stable *S1PR3* knock-down cell lines were established via lentivirus-mediated gene transfer. After stable growth was achieved, the extent of *S1PR3* silencing was verified by qPCR and western blotting analyses.

#### Western blotting analysis

After collection, the cells were lysed in a lysis buffer (Epizyme Biomedical Technology Co., Ltd., Shanghai, China), and total protein was evaluated with a bicinchoninic acid assay kit (Beyotime Biotechnology, Shanghai, China). Equal quantities of total protein samples were submitted to electrophoresis in 10% polyacrylamide gels and subsequently moved to polyvinylidene fluoride membranes (Bio-Rad Laboratories, Inc., CA, USA). The aforementioned membranes were treated at ambient temperature for 1 h with rapid blocking buffer (Epizyme) to inhibit non-specific binding and then exposed overnight to primary antibodies. Next, membranes were treated with secondary antibodies at ambient temperature for 1 h. Employing an enhanced chemiluminescence reagent (Epizyme), signals were detected following the manufacturer's guidelines.

#### Cell counting kit-8 (CCK-8) and colony formation assays

OSCC cells (5000/well) were plated into 96-well plates. After treatment, cultures were terminated at designated time points, and plates were placed in a cell incubator for 2 h after adding CCK8 solution (10 μL/well, Dojindo Laboratories Co., Ltd., Kumamoto, Japan). Cell viability was determined from absorbance at 450 nm, measured by a microplate reader (Bio-Rad Laboratories, CA, USA).

OSCC cells (800/well) were plated into 6-well plates. After treatment, cultures were terminated at specified time points, followed by the addition of 4% paraformaldehyde (1 mL/well) for cell fixation for 30 min. After washing once with PBS, 1% crystal violet staining solution was deposited into wells, and then subjected to a 30-min incubation at room temperature. Cells were rinsed with running water and left to air dry. Afterward, photographs of the cells were taken, and the cell colony count was performed.

#### Cell proliferation assay

OSCC cells ( $1 \times 10^5$ /well) were plated into 12-well plates. After treatment, cultures were terminated at designated time points. DNA replication was assessed with the

5-ethynyl-2'-deoxyuridine (EdU) detection kit (Beyotime). EdU-positive cells were subsequently observed with a fluorescence microscope (Olympus, Tokyo, Japan).

#### Cell cycle analysis

*S1PR3* knockdown CAL27 cells, along with control cells, were plated in 6-well plates and kept in a cell incubator for three days. Cells from each experimental group were collected in flow cytometry tubes for cell cycle analysis. OSCC cells were plated into 6-well plates and treated with 0  $\mu$ M, 300  $\mu$ M, or 400  $\mu$ M CAY10444 for 24 h. Pre-cooled 70% ethanol solution was added to flow cytometry tubes to fix cells overnight. Following the addition of PI/RNase staining buffer, cells were stained in accordance with the manufacturer's guidelines, and the cell cycle profile was analyzed in a flow cytometer (BD FACSCanto II, CA, USA).

#### RNA-seq analysis

Following RNA isolation from OSCC cells using TRIzol reagent (Invitrogen), RNA-seq libraries were generated with the Ovation Universal RNA-Seq System 1–16 (NuGEN Technologies, Inc., CA, USA). The indexed libraries were multiplexed in a single flow cell and sequenced using 75-base pair single-end reads on a Next-Seq 500 High Output Kit v2 (75 cycles; Illumina, Inc., CA, USA), performed by BGI Group (Beijing, China).

#### Prediction analysis of immunotherapy responsiveness

To evaluate immunotherapy responsiveness in the TCGA HNSCC cohort, TIDE scores and Immune Prognostic Scores (IPS) were calculated for each patient.

#### Analysis of targeted agents sensitivity

The "oncopredict" R package was used to estimate the  $IC_{50}$  values of targeted agents in HNSCC patients with high or low *S1PR3* expression. This analysis aimed to evaluate their differential sensitivity to pharmacological treatments.

#### Cell apoptosis analysis

Cell apoptosis was assessed using Annexin V-FITC/PI dual staining. Following treatment, cells were harvested, washed twice with cold PBS, and resuspended in binding buffer. Subsequently, 5  $\mu$ L of Annexin V-FITC and 5  $\mu$ L of PI were added, and the cells were incubated at room temperature in the dark for 15 min. Apoptosis was then analyzed using a flow cytometer (BD FACSCanto II, CA, USA).

#### $\gamma$ -H2 AX immunofluorescence

CAL27 cells were seeded in 6-well plates and treated with the indicated drugs. At the designated time points,

the culture was terminated. Cells were washed with PBS and fixed for 15 min, followed by three washes. After blocking at room temperature for 20 min, cells were incubated with anti- $\gamma$ -H2 AX primary antibody at 4 °C overnight and then washed three times. Subsequently, cells were incubated with Alexa Fluor 488-conjugated anti-rabbit secondary antibody for 1 h at room temperature, followed by two washes. Fluorescence signals were observed and imaged under a fluorescence microscope (Olympus, Tokyo, Japan), with  $\gamma$ -H2 AX appearing as green fluorescence.

#### Statistical analysis

Statistical analyses were performed with GraphPad Prism 8.0.2 software. Chi-square test or Fisher's exact test was used to assess correlations between *S1PR3* expression and clinicopathological features. Pairwise comparisons were conducted using the two-tailed Student's t-test. Multiple group comparisons were carried out using one-way or two-way ANOVA. The results were expressed as mean  $\pm$  standard deviation, and the level of statistical significance was considered according to the p values obtained (i.e., <0.05, <0.01, or <0.001).

## Results

### The overexpression of *S1PR3* is correlated with poor prognosis in OSCC patients

S1PRs have been found to show altered expression in various cancers and influence cancer progression [11]. Thus, we examined S1PR expression levels in HaCat, HNSCC cell lines using qPCR and western blotting analyses. The findings revealed that S1PR1, S1PR3 and S1PR4 were upregulated in HNSCC cell lines, with S1PR3 exhibiting higher expression in most HNSCC cell lines compared to the other S1PRs (Supplementary Fig. 1A, B). Subsequently, HNSCC transcriptome sequencing data retrieved from the TCGA database were employed to assess the clinical relevance of *S1PR3* mRNA levels in HNSCC. The data revealed that *S1PR3* was abnormally upregulated in HNSCC tissues when contrasted with normal tissues (Fig. 1A, B). Additionally, we performed IHC staining to confirm S1PR3 expression in human tissues. The findings indicated that S1PR3 exhibited elevated expression in clinical OSCC tissues relative to adjacent tissues (Fig. 1C). Importantly, elevated levels of S1PR3 expression correlated with advanced pathological stages in HNSCC patients (Fig. 1D, E).

Furthermore, the association between S1PR3 levels and clinicopathological characteristics among 52 OSCC patients was thoroughly examined. After the quantification of IHC images, it was demonstrated that S1PR3 expression was markedly elevated in stage III/IV tumors when contrasted with stage I/II tumors (Fig. 1F, G).



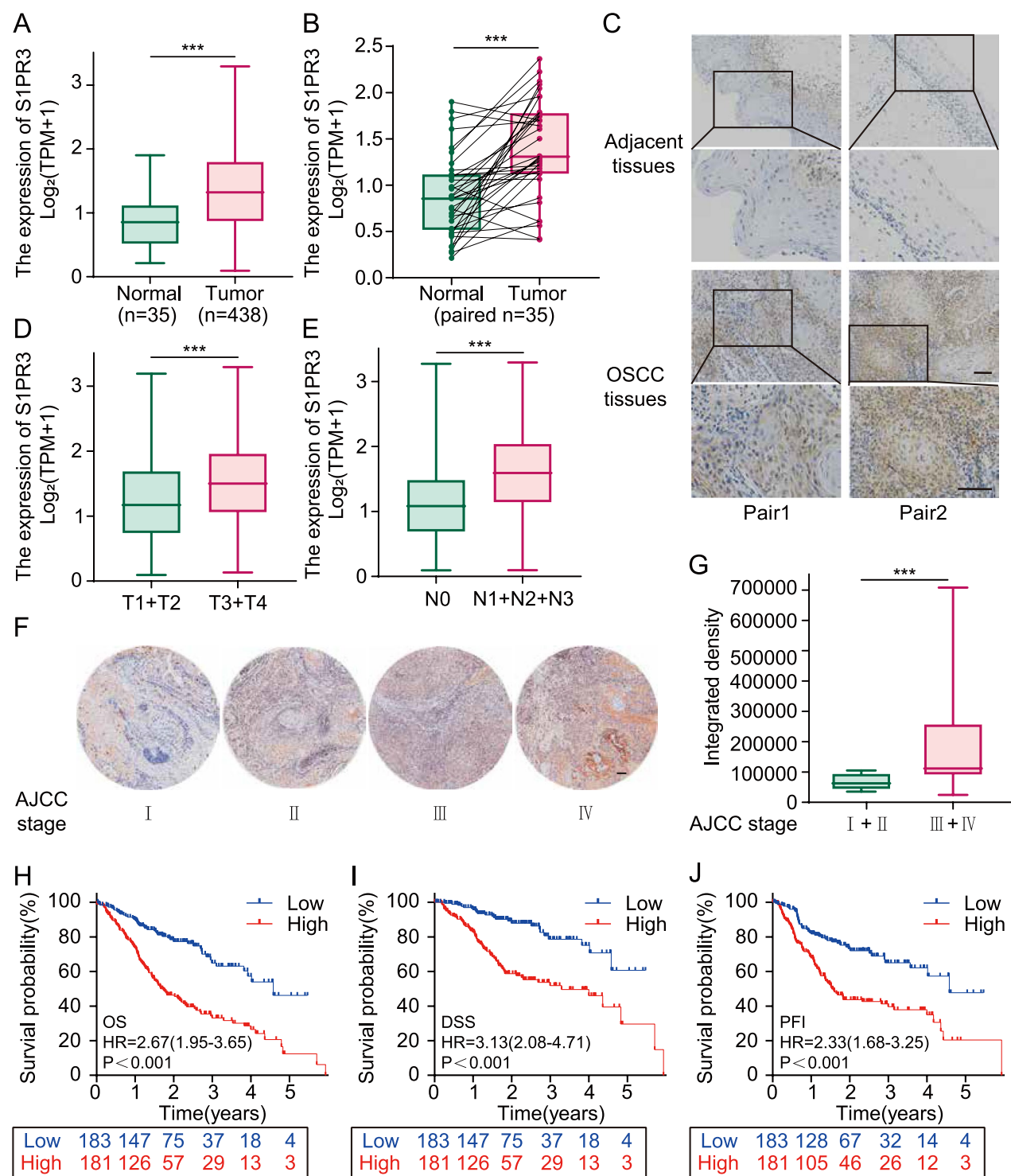


**Fig. 1** The overexpression of *S1PR3* was correlated with poor prognosis in OSCC patients. **A, B** Analysis of *S1PR3* mRNA levels in HNSCC patients according to the TCGA database. *S1PR3* mRNA levels were markedly increased in HNSCC tissues (**A**). *S1PR3* expression in HNSCC was higher compared to the matched normal samples (**B**). **C** *S1PR3* expression patterns in OSCC tissues and adjacent tissues were identified through IHC staining. **D, E** Analysis of *S1PR3* mRNA levels in HNSCC patients according to the TCGA database. Upregulated *S1PR3* expression demonstrated a significant association with T (**D**) and N stage (**E**). **F, G** The relationship between *S1PR3* protein levels and clinicopathological characteristics was observed in 52 OSCC patients. **H–J** Survival analysis of the correlations between *S1PR3* mRNA levels and OS, DSS and PFI of HNSCC patients using TCGA database. Data were presented as mean ± SD, with n = 3 biological replicates. \*\*\*P < 0.001. Scale bar, 100 μm

Moreover, *S1PR3* upregulation was significantly associated with AJCC ( $P < 0.001$ ), T ( $P < 0.05$ ) and N stages ( $P < 0.05$ ) in OSCC patients (Table 1). Subsequently, the predictive value of *S1PR3* in HNSCC patients was investigated. As shown in Fig. 1H–J, among the *S1PR* family, only high *S1PR3* expression exhibited a negative correlation with patient prognosis. In particular, HNSCC patients with higher *S1PR3* expression had shorter OS (HR = 2.67,  $P < 0.001$ ), DSS (HR = 3.13,  $P < 0.001$ ) and PFI (HR = 2.33,  $P < 0.001$ ). In addition, afatinib is a second-generation EGFR TKI inhibitor that is used as a second-line treatment for recurrent or metastatic HNSCC [12]. The analysis of TCGA data showed that high *S1PR3*

expression was associated with higher afatinib  $IC_{50}$  values, increased TIDE scores and reduced IPS (Supplementary Fig. 2A–C). Therefore, *S1PR3* was found to promote OSCC progression, thus playing a crucial role in predicting clinical outcomes in OSCC patients.

### S1PR3 inhibition suppresses OSCC cell growth

Based on the above-discussed observations, *S1PR3* was frequently overexpressed in OSCC, which might contribute to tumor initiation and progression. Therefore, we constructed two lentiviral plasmids, *S1PR3*-SH1 and *S1PR3*-SH2, to achieve *S1PR3* knockdown and thereby explore the impact of *S1PR3* on the biological functions of OSCC cells. Furthermore, CAL27 cells were selected to establish stable knockdown cell lines due to their elevated *S1PR3* expression. The efficiency of knockdown was verified by qPCR (Fig. 2A) and western blotting analyses (Fig. 2B).

CCK8 and colony formation assays were subsequently performed to examine the impact of *S1PR3* inhibition on OSCC cell proliferation. The analysis showed that viability and colony count of OSCC cells were notably decreased by *S1PR3* knockdown (Fig. 2C, D). To further validate these observations, OSCC cells were treated with the specific an *S1PR3* antagonist, CAY10444, which suppressed OSCC cell growth in a dose-dependent way (Fig. 2E, F). In addition, the results of CCK8 assay demonstrated that inhibiting *S1PR3* significantly suppressed the growth of human laryngeal squamous cell carcinoma cell line WSU-HN4 cells (Supplementary Fig. 3A). Therefore, targeting *S1PR3* via shRNA or by using a specific antagonist effectively suppressed malignancy of OSCC cells.

### S1PR3 inhibition suppresses OSCC cell proliferation by regulating the cell cycle

The EdU incorporation assay was conducted to evaluate whether reduced *S1PR3* expression inhibited OSCC cell proliferation. The analysis demonstrated that the knockdown of *S1PR3* in CAL27 cells decreased EdU-positive rates, dropping from  $35.64\% \pm 3.46\%$  to  $22.62\% \pm 2.69\%$  or  $18.87\% \pm 2.72\%$  (Fig. 3A and Supplementary Fig. 4A), indicating a suppressive effect of *S1PR3* knockdown on cell proliferation. Comparable findings were

**Table 1** Correlation between *S1PR3* expression and clinicopathological features in patients with OSCC (n = 52)

	Number(52)	S1PR3 expression		P value
		Low	High	
Age				
< 60	32	14	18	0.393
≥ 60	20	12	8	
Gender				
Male	43	23	20	0.465
Female	9	3	6	
Location				
Tongue	30	14	16	0.532
Gingiva	4	2	2	
Pharynx oralis	13	8	5	
Palatal	2	0	2	
Others	3	2	1	
AJCC stage				
I	3	3	0	$P < 0.01$
II	7	7	0	
III	32	14	18	
IV	10	2	8	
T stage				
T1 + T2	32	20	12	$P < 0.05$
T3 + T4	20	6	14	
N stage				
N0	23	16	7	$P < 0.05$
N1 + N2	29	10	19	

(See figure on next page.)

**Fig. 2** *S1PR3* inhibition suppressed OSCC cell growth. **A**, **B** Establishment of *S1PR3* knockdown CAL27 cell lines. The efficiency of knockdown was verified using qPCR (**A**) and western blotting analysis (**B**). **C** Cell viability of *S1PR3* knockdown and control CAL27 cells was evaluated by the CCK8 assay. **D** Colony-forming ability of *S1PR3* knockdown and control CAL27 cells was evaluated by the colony formation assay. **E** The results of the CCK8 assay indicated that the *S1PR3* antagonist inhibited the viability of CAL27 and WSU-HN30 cells in a dose-dependent manner (25  $\mu$ M, 50  $\mu$ M, 100  $\mu$ M, 200  $\mu$ M, 300  $\mu$ M and 400  $\mu$ M vs 0  $\mu$ M). **F** The results of the colony formation assay indicated that the *S1PR3* antagonist inhibited the colony-forming ability of CAL27 and WSU-HN30 cells in a dose-dependent manner (25  $\mu$ M, 50  $\mu$ M, 100  $\mu$ M, 200  $\mu$ M, 300  $\mu$ M and 400  $\mu$ M vs 0  $\mu$ M). Data were presented as mean  $\pm$  SD, with n = 3 biological replicates. \*\* $P < 0.01$ , \*\*\* $P < 0.001$

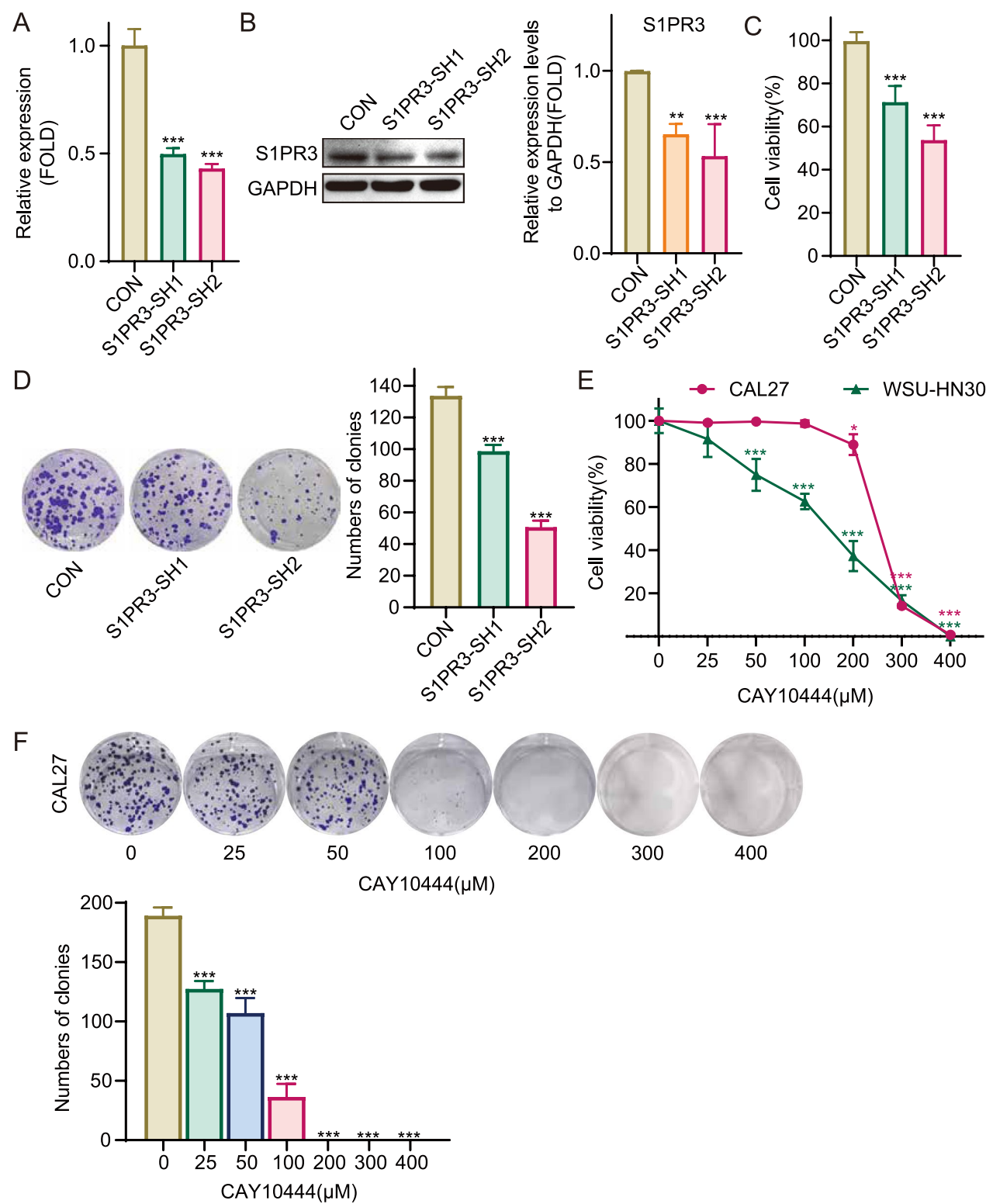


**Fig. 2** (See legend on previous page.)

noted in OSCC cells subjected to the *S1PR3* antagonist (Fig. 3B and Supplementary Fig. 4B). CAL27 and WSU-HN30 cells were subjected to the antagonist CAY10444 at a range of concentrations. In CAL27 cells, treatment with 300  $\mu$ M CAY10444 reduced the EdU-positive rate to  $3.00\% \pm 0.70\%$ , with a further decrease to  $0.53\% \pm 0.40\%$  when treated with 400  $\mu$ M CAY10444, in comparison with the control group rate of  $32.47\% \pm 5.04\%$ . A similar trend was noted in WSU-HN30 cells.

To better elucidate the role of *S1PR3* in OSCC, KEGG enrichment analysis of RNA-seq results was conducted, and the top 20 statistically significantly enriched functional entries were identified. Among these, cell cycle-related genes were particularly enriched in the CAY10444 treatment group (Fig. 3C), suggesting that *S1PR3* inhibition might hinder the proliferation of OSCC cells via regulation of cell cycle. Subsequently, we evaluated the effect of *S1PR3* inhibition on the distribution of the OSCC cell cycle. As shown in Fig. 3D and E, the percentage of cells in the S phase significantly decreased, while the percentage of cells in the G2/M phase increased after *S1PR3* knockdown or antagonist treatment. This indicates that *S1PR3* intervention led to a modification in cell cycle regulation. Hence, it can be hypothesized that *S1PR3* intervention inhibits cell proliferation by regulating OSCC cell cycle.

### ***S1PR3* inhibition modulates OSCC cell cycle by reducing *WEE1* expression**

To analyse the molecular basis driving the impact of *S1PR3* inhibition on the OSCC cell cycle, a qPCR array targeting 90 cell cycle-related genes was performed. The findings indicated that four genes, i.e., *WEE1*, *GADD45 A*, *CDKN1 A* and *CCNA1*, were differentially expressed after treatment with CAY10444 compared to control CAL27 cells. *WEE1* was downregulated, while *GADD45 A*, *CDKN1 A* and *CCNA1* were upregulated (Fig. 4A, B). The transcription levels of these four genes were further validated using qPCR, confirming that *WEE1* transcription was downregulated in the *S1PR3* knockdown group and the presence of the antagonist (Fig. 4C). *WEE1*, a gene encoding a protein within the serine/threonine kinase family, regulates CDC2 activity via

phosphorylation. *WEE1* downregulation disrupts the G2/M checkpoint by reducing CDC2 phosphorylation, thereby modulating the cell cycle [13]. Therefore, we further examined *WEE1* expression and CDC2 phosphorylation via western blotting analysis. The findings revealed that both *WEE1* expression and CDC2 phosphorylation were decreased in *S1PR3* knockdown and antagonist-treated OSCC cells (Fig. 4D, E). Thus, it was hypothesized that *S1PR3* inhibition might modulate the OSCC cell cycle by downregulating *WEE1* expression.

### ***S1PR3* inhibition downregulates *WEE1* expression by regulating the AKT signaling pathway**

Subsequently, gene clustering analysis was used to identify signaling pathways affected by both CAY10444 treatment or *S1PR3* knockdown. Compared to control CAL27 cells, the findings indicated that treatment with CAY10444 modulated several signaling pathways, including PI3 K/AKT, PI3 K/AKT/mTOR and MAPK. However, the most significant impact was observed on the PI3 K/AKT signaling pathway (Supplementary Fig. 5A). Importantly, the PI3 K/AKT signaling pathway was the only pathway commonly regulated by both CAY10444 treatment and *S1PR3* knockdown (Fig. 5A). The PI3 K/AKT signaling pathway is essential for regulating cell survival, metastasis and apoptosis, thereby contributing to tumor progression [14–19]. Previous research has indicated that *S1PR3* activates various pathways, including the PI3 K/AKT signaling pathway, by binding specifically to  $G_i$  [20].

To further determine whether inhibiting *S1PR3* expression in OSCC cells affects the PI3 K/AKT signaling pathway, we analyzed the phosphorylation levels of AKT in tumor cells after *S1PR3* knockdown and antagonist treatment and protein levels of the involved molecules were measured via western blotting analysis. The data revealed that both *S1PR3* knockdown and antagonist treatment inhibited AKT phosphorylation (Fig. 5B, C). Therefore, it could be hypothesized that inhibiting *S1PR3* might downregulate the abundance of *WEE1* by the AKT signaling pathway. Thus, we further evaluated whether an AKT agonist could reverse the growth inhibition effect of targeting *S1PR3* in OSCC cells. Based on western blotting results, SC79 was found to increase AKT

(See figure on next page.)

**Fig. 3** *S1PR3* inhibition suppressed OSCC cell proliferation by regulating the cell cycle. **A** The proliferative ability of the knockdown and control CAL27 cells was detected using the EdU incorporation assay at designated time points. **B** Following treatment with 0  $\mu$ M, 300  $\mu$ M, or 400  $\mu$ M CAY10444, the proliferation of CAL27 and WSU-HN30 cells was evaluated using the EdU incorporation assay. **C** RNA sequencing was conducted on CAY10444-treated and control CAL27 cells, followed by KEGG enrichment analysis to reveal the mechanism by which CAY10444 restrains OSCC cell growth. **D** The PI staining and flow cytometry were used to assess the cell cycle phases in *S1PR3* knockdown and control CAL27 cells. **E** Following treatment with 0  $\mu$ M, 300  $\mu$ M, or 400  $\mu$ M CAY10444, the PI staining and flow cytometry were used to assess the cell cycle phases in CAL27 and WSU-HN30 cells. Data were presented as mean  $\pm$  SD, with  $n = 3$  biological replicates. \* $P < 0.05$ , \*\* $P < 0.01$ , \*\*\* $P < 0.001$



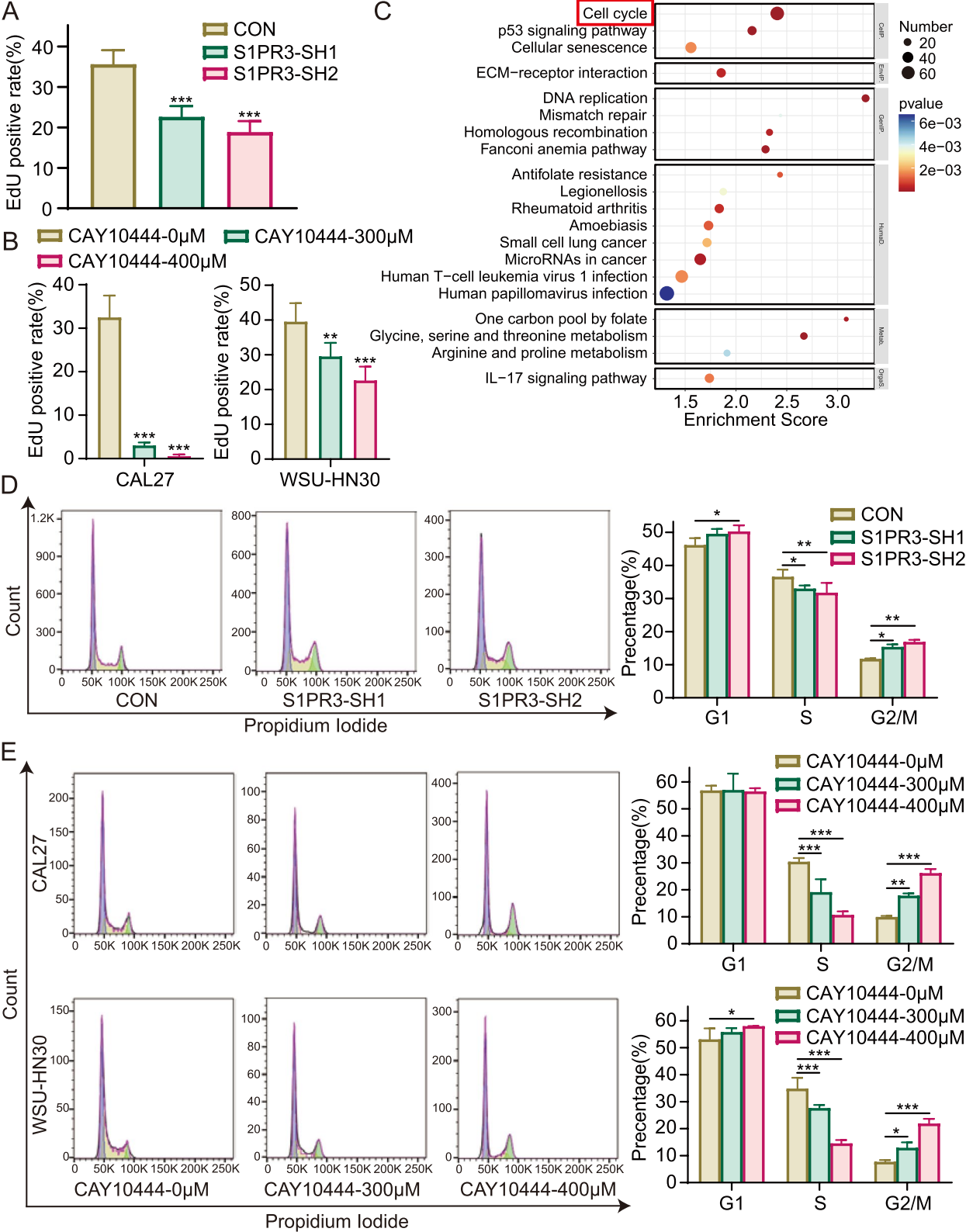


**Fig. 3** (See legend on previous page.)

phosphorylation levels (Supplementary Fig. 6A). Moreover, the CCK8 assay showed that the AKT agonist SC79 partly mitigated the repressive effect of *S1PR3* knockdown and antagonist treatment on OSCC cell growth (Fig. 5D, E). As shown in Fig. 5F, SC79 significantly upregulated WEE1 expression and CDC2 phosphorylation in *S1PR3* antagonist-treated OSCC cells. Thus, these findings suggest that the AKT/WEE1/CDC2 axis mediates the growth inhibition effect of *S1PR3* inhibition in OSCC cells.

### ***S1PR3* inhibition suppresses OSCC cell growth via AKT signaling pathway in vivo**

We established a cell line-derived xenograft model to validate the growth-inhibitory effect of targeting *S1PR3* on OSCC cells. No notable adverse effects were detected in mice following injection with *S1PR3* knockdown cells (Supplementary Fig. 7A). Moreover, the injection of stable *S1PR3* knockdown cells into mice led to a marked delay in tumor growth, with both tumor volume and weight substantially reduced (Fig. 6A–C).

Additionally, the effect of *S1PR3* knockdown on expression of *S1PR3*, p-AKT, WEE1 and Ki67 was appraised in vivo using IHC staining. In alignment with in vitro results, expression of *S1PR3*, p-AKT and WEE1 were substantially decreased among mice injected with *S1PR3* knockdown groups, and OSCC cell proliferation was inhibited (Fig. 6D). In summary, these findings indicate that *S1PR3* knockdown inhibited OSCC cell expansion in vivo.

Furthermore, to determine whether targeting *S1PR3* curbs OSCC cell growth in vivo via the AKT signaling pathway, mice with xenograft tumors after injection of *S1PR3* knockdown cells and control CAL27 cells were further divided into drug treatment and non-treatment groups. SC79 was administered intraperitoneally to the treatment group, while the non-treatment group received an equivalent amount of DMSO. Consistent with previous experimental results, No notable adverse effects were detected in mice following injection with *S1PR3* knockdown cells (Supplementary Fig. 7B). As shown in Fig. 6E–G, mice injected with stable *S1PR3* knockdown cells showed significantly reduced tumor volume and weight.

Notably, SC79 markedly attenuated tumor suppression induced by injection with *S1PR3* knockdown cells.

In addition, we examined the expression of *S1PR3*, p-AKT, WEE1 and Ki67 in xenograft tumors from each group using IHC staining. The expression of p-AKT, WEE1 and Ki67 were markedly decreased among mice injected with *S1PR3* knockdown cells, an effect which was reversed by treatment with SC79 (Fig. 6H). Thus, the results of in vivo experiments further demonstrate that *S1PR3* promotes OSCC progression by regulating the AKT signaling pathway.

### ***S1PR3* antagonist combined with cisplatin suppresses OSCC cells growth**

Cisplatin (CDDP) is a widely used chemotherapeutic drug for OSCC treatment and exerts its antitumor effect by disrupting the structure and function of tumor cell DNA [21, 22]. Therefore, the impact of treatment with *S1PR3* antagonist CAY10444 on the antitumor effects of CDDP in OSCC cells was evaluated. It was found that treatment with either CDDP or CAY10444 inhibited OSCC cell viability, and when used in combination, the inhibitory effect was further exacerbated (Fig. 7A, B). Moreover, using the EdU incorporation assay, it was further revealed that the combination of CDDP and CAY10444 significantly inhibited OSCC cell proliferation compared to their effect when employed alone (Fig. 7C, D). Additionally, the apoptosis assay and  $\gamma$ -H2 AX detection indicated that the combination of the *S1PR3* antagonist and CDDP promotes apoptosis (Supplementary Fig. 8A) and enhances DNA damage (Supplementary Fig. 8B). Collectively, these data imply that combining CDDP with CAY10444 may result in enhanced therapeutic benefits.

### **Discussion**

It is known that *S1PRs* display differential expression patterns in different types of tumors, significantly influencing tumor progression. For instance, *S1PR1* is upregulated in breast and ovarian cancers [23]. However, *S1PR2* expression varies by tumor type, showing high levels in pancreatic cancer but low levels in gastric and colorectal cancers [24–26]. *S1PR3* is upregulated in various tumors, including osteosarcoma, lung adenocarcinoma and breast

(See figure on next page.)

**Fig. 4** *S1PR3* inhibition modulated OSCC cell cycle by reducing WEE1 expression. **A, B** The mRNA levels of genes associated with the cell cycle in *S1PR3* antagonist-treated CAL27 cells were analyzed using a qPCR-based cell cycle array. **C** The mRNA levels of differentially expressed genes in *S1PR3* knockdown and antagonist-treated CAL27 cells were validated using qPCR. **D** Western blotting analysis revealed the translational levels of *S1PR3*, WEE1, CDC2 and p-CDC2 in CAY10444-treated CAL27 and WSU-HN30 cells. **E** Western blotting analysis revealed the translational levels of *S1PR3*, WEE1, CDC2 and p-CDC2 in *S1PR3* knockdown and control CAL27 cells. Data were presented as mean  $\pm$  SD, with  $n = 3$  biological replicates. \* $P < 0.05$ , \*\* $P < 0.01$ , \*\*\* $P < 0.001$

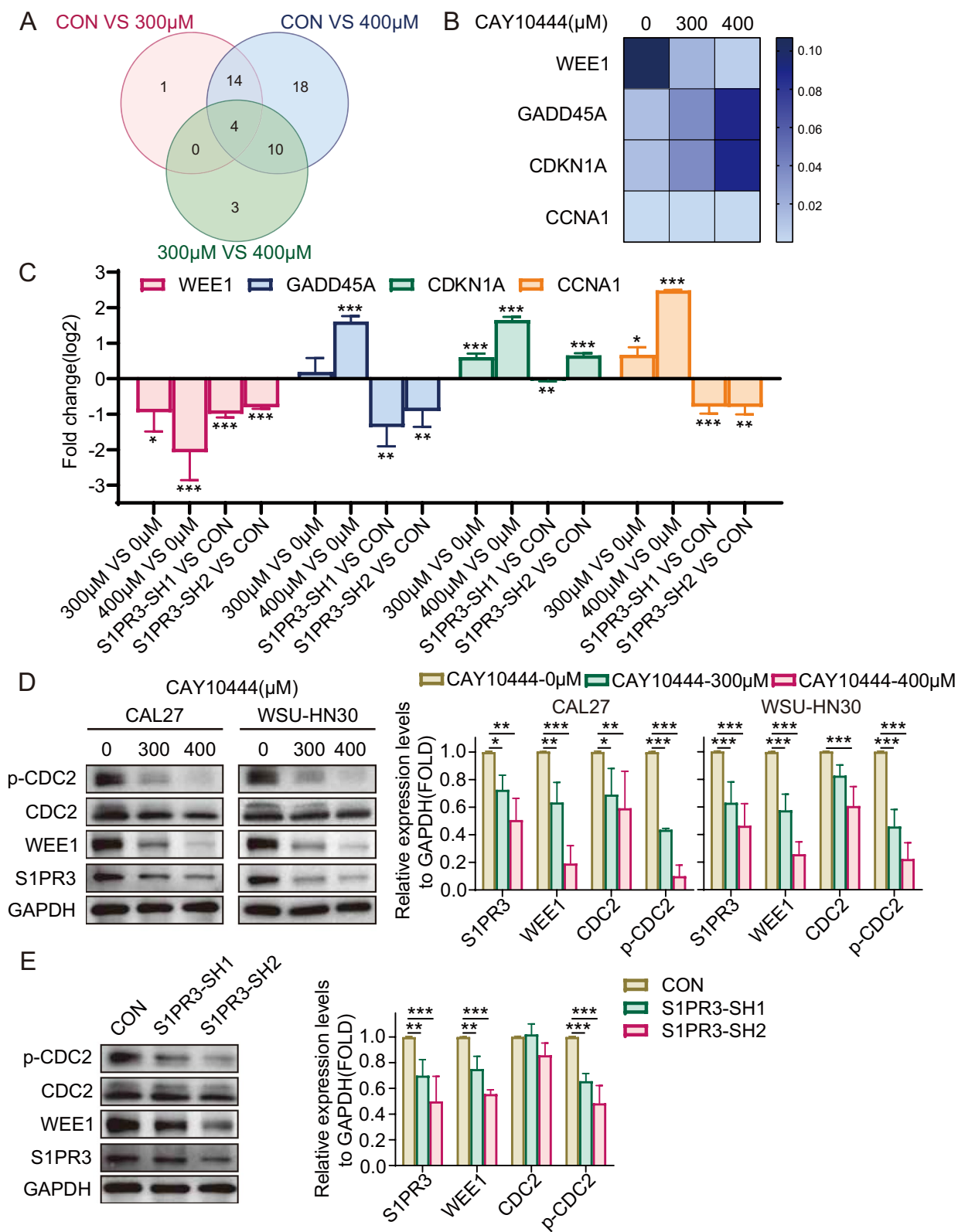


**Fig. 4** (See legend on previous page.)

cancer, being linked to poor prognosis in cancer patients [27–29]. A clinical study reported that S1PR4 expression levels are elevated in ER-negative breast cancer and show a negative correlation with disease-free survival [30]. Research indicates that the protein levels of S1PR5 are reduced in esophageal squamous cell carcinoma [9]. However, the transcriptional and translational levels of S1PRs in OSCC have not been fully elucidated. In this study, S1PR1, S1PR3 and S1PR4 were found upregulated in most OSCC cells. Inhibition of S1PR3 may lead to compensatory activation of other receptors. The results of qPCR validation showed that *S1PR1* was upregulated after inhibition of S1PR3 (Supplementary Fig. 9A). The combination of S1PR1 and S1PR3 antagonist enhanced the inhibitory effects on OSCC cell growth (Supplementary Fig. 9B). In addition, *S1PR3* was the only *S1PR* correlated with unfavorable prognosis in HNSCC patients. In recent years, there has been rapid development in computational algorithms and bioinformatics [39–42]. The analysis of TCGA database showed that HNSCC patients exhibiting higher *S1PR3* expression tended to be found in more advanced clinical stages of the disease and to exhibit worse OS, DSS and PFI. Additionally, this study found that high S1PR3 expression was associated with reduced sensitivity to afatinib, which is a second-line treatment for recurrent or metastatic HNSCC [12]. IPS and TIDE scores, key indicators of immunotherapy response, showed that the high S1PR3 expression group had significantly lower IPS, decreased tumor suppressor cell infiltration and higher TIDE scores. Moreover, T cell exclusion and CAF infiltration were significantly increased, while MSI scores were lower in this group. These findings suggested that patients with high S1PR3 expression have lower immunotherapy responsiveness. S1PR3 has been implicated in tumor progression, significantly affecting key biological processes in tumoral cells including proliferation, apoptosis, invasion and migration. The S1P/S1PR3 signaling pathway enhances aerobic glycolysis in osteosarcoma cells, suppressing apoptosis and promoting cell proliferation [27]. Additionally, it has been shown that high S1PR3 expression enhances invasion and migration in gastric carcinoma cells [10]. The findings of this study showed that the inhibition of

S1PR3 significantly attenuated the proliferative capacity of OSCC and LSCC cells, which provided a more comprehensive understanding of the role of S1PR3 in head and neck cancers. Moreover, *S1PR3* knockdown or antagonist-mediated inhibition suppressed OSCC cell proliferation by regulating the cell cycle, thereby exerting antitumor effects.

In order to investigate how S1PR3 regulates the OSCC cell cycle, a qPCR-based cell cycle array was employed to identify differentially expressed genes after treatment with the S1PR3 antagonist. *WEE1* was identified as the most significantly downregulated gene. *WEE1* encodes a tyrosine/threonine protein kinase that is crucial for regulating the cell cycle and repairing DNA damage. *WEE1* primarily inhibits the activity of the G2/M phase regulatory protein CDC2 by phosphorylating it. Thus, downregulation of *WEE1* can lead to G2/M checkpoint dysregulation, thereby affecting the cell cycle and further inhibiting tumor cell growth. A previous study described that inhibiting *WEE1* expression via small interfering RNA (siRNA) increased the percentage of melanoma cells in the G2/M transition phase, thereby inhibiting cell proliferation [31]. Another study reported that adding a *WEE1* inhibitor to drug-resistant breast cancer cells resulted in prolongation of the G2/M phase, which significantly inhibited tumor proliferation and induced apoptosis [32]. Similarly, the findings discussed herein showed that downregulation of *WEE1* inhibited CDC2 phosphorylation in OSCC, leading to G2/M checkpoint failure and thereby affecting the cell cycle.

Gene clustering functional analysis was employed to identify signaling pathways impacted by CAY10444 treatment and *S1PR3* knockdown, aiming to explore the molecular pathway by which targeting *S1PR3* affects *WEE1* expression. The results indicated that although CAY10444 treatment affected the PI3 K/AKT, PI3 K/AKT/mTOR and MAPK signaling pathways, the PI3 K/AKT signaling pathway was the only common pathway influenced by both treatments. Studies have reported that S1PR3 can bind to multiple  $G_\alpha$  proteins, including  $G_i$ ,  $G_q$  and  $G_{12/13}$ , thus modulating signaling pathways such as AC/cAMP, Ras/ERK/AC, PI3 K/AKT, PLC/ $Ca^{2+}$  and Rho/ROCK [20]. Therefore, it can be hypothesized

(See figure on next page.)

**Fig. 5** S1PR3 blockade downregulated *WEE1* expression via regulating the AKT signaling pathway. **A** The signaling pathways that exhibited statistically significant differences after S1PR3 antagonist treatment and *S1PR3* knockdown compared to control CAL27 cells were identified by RNA-seq. **B** The translational levels of S1PR3, p-AKT and AKT in *S1PR3* knockdown and control CAL27 cells were measured using western blotting analyses. **C** The translational levels of S1PR3, p-AKT and AKT in S1PR3 antagonist-treated CAL27 and WSU-HN30 cells were measured using western blotting analyses. **D** OSCC cell viability in different groups (control, CAY10444, SC79, CAY10444 + SC79) was measured by the CCK8 assay. **E** Following SC79 treatment or non-treatment, the viability of *S1PR3* knockdown and control CAL27 cells was measured by the CCK8 assay. **F** The translational levels of S1PR3, AKT, p-AKT, *WEE1*, CDC2 and p-CDC2 in OSCC cells from different groups (control, CAY10444, SC79, CAY10444 + SC79) were measured by western blotting analyses. Data were presented as mean  $\pm$  SD, with  $n = 3$  biological replicates. \* $P < 0.05$ , \*\* $P < 0.01$ , \*\*\* $P < 0.001$





that targeting *S1PR3* in OSCC can inhibit the activation of the PI3 K/AKT signaling pathway. The PI3 K/AKT signaling pathway has very important biological functions in tumors [33–35]. The results confirmed that inhibiting *S1PR3* resulted in decreased AKT phosphorylation levels. In contrast, the AKT agonist SC79 restored the inhibitory effect on OSCC cell growth caused by *S1PR3* inhibition both in vitro and in vivo. Furthermore, SC79 partially reversed the downregulation of WEE1 and p-CDC2 induced by targeting *S1PR3*. Collectively, these findings indicated that *S1PR3* knockdown inhibited OSCC cell growth through modulating the AKT/WEE1 signaling pathway.

CDDP is a widely used chemotherapeutic agent, known for its strong antitumor activity against various cancers, and remains the first-line treatment for OSCC. In fact, adjuvant cisplatin therapy administered pre- or postoperatively enhanced the prognosis of OSCC patients [36, 37]. However, the extensive use of cisplatin in more recent years has contributed to the development of chemotherapy resistance, substantially reducing its effectiveness in OSCC treatment. Therefore, improving or reestablishing tumor cell sensitivity to cisplatin has become a critical research direction for enhancing chemotherapy efficacy. Furthermore, AKT activation has been closely tied to cisplatin resistance in lung cancer, with AKT1 driving the chemoresistance in tumor cells via the mTOR signaling pathway [38]. Our findings in this study showed that the combination of cisplatin and the *S1PR3* antagonist enhanced the inhibition of the malignant biological behaviors of OSCC cells. Herein, *S1PR3* antagonists were found to significantly enhance the suppressive influence of cisplatin on OSCC cell growth by increasing apoptosis induction and DNA damage, as well as regulating cell cycle. Additionally, the AKT signaling pathway was confirmed to function as a key downstream effector

of *S1PR3*. Although our findings indicated that *S1PR3* antagonist enhanced the cytotoxic effects of cisplatin on OSCC cells, the underlying mechanisms remain to be fully elucidated. Moreover, the immunomodulatory roles of *S1PR3* antagonist and its clinical therapeutic potential require further investigation and validation through additional experimental and clinical data.

Recent insights into *S1PRs* as therapeutic targets for enhancing antitumor drug sensitivity have garnered considerable attention. Fingolimod (FTY720), a modulator of *S1PRs* (including *S1PR3*), has shown efficacy in reversing trastuzumab resistance in HER2-positive breast cancer patients [43]. In colon cancer, FTY720 has been shown to enhance tumor cell chemosensitivity to doxorubicin and etoposide by modulating P-glycoprotein and multidrug resistance protein 1 [44]. Therefore, *S1PR3* could represent a potential therapeutic target to increase OSCC cell sensitivity to cisplatin.

Hence, the findings discussed herein revealed that targeting *S1PR3* could regulate OSCC cell cycle by modulating the AKT/WEE1 signaling pathway, thereby inhibiting OSCC cell proliferation (Fig. 8). Furthermore, it was found that the specific *S1PR3* antagonist CAY10444 exhibited a synergetic effect with cisplatin to inhibit OSCC cell growth, providing new insights into the clinical treatment of OSCC. Therefore, targeting the *S1PR3*/AKT/WEE1 signaling pathway might represent a novel therapeutic strategy for OSCC. However, the therapeutic effects of targeting *S1PR3* require further clinical studies.

## Conclusions

These findings reveal a critical role for *S1PR3* in regulating OSCC cell cycle via the AKT/WEE1/CDC2 pathway, thus offering a basis for developing treatment strategies for OSCC patients.

(See figure on next page.)

**Fig. 6** *S1PR3* inhibition suppressed OSCC cell growth via AKT signaling pathway in vivo. **A–C** The xenograft tumor model using *S1PR3* knockdown or control CAL27 cells was established in the groin of nude mice. Volumes of xenograft tumors (**A**) were evaluated every 5 days. The tumors of each group were excised and photographed after 20 days. Tumor images (**B**) and weights (**C**) were then evaluated. **D** The translational levels of *S1PR3*, p-AKT, WEE1 and Ki67 in the xenograft tumors were analyzed through IHC staining. **E–G** The xenograft tumor models using *S1PR3* knockdown and control CAL27 cells were established and randomly divided into treatment and non-treatment groups. SC79 was administered to the treatment group every 3 days at a concentration of 20 mg/kg, while the non-treatment group received an equivalent volume of DMSO. Volumes of xenograft tumors (**E**) were evaluated every 3 days. The tumors of each group were excised and photographed after 12 days. Tumor images (**F**) and weights (**G**) were then evaluated. **H** The translational levels of *S1PR3*, p-AKT, WEE1 and Ki67 in the xenograft tumors were analyzed through IHC staining. Data were presented as mean  $\pm$  SD, with  $n = 3$  biological replicates. \* $P < 0.05$ , \*\*\* $P < 0.001$ . Scale bar, 100  $\mu$ m

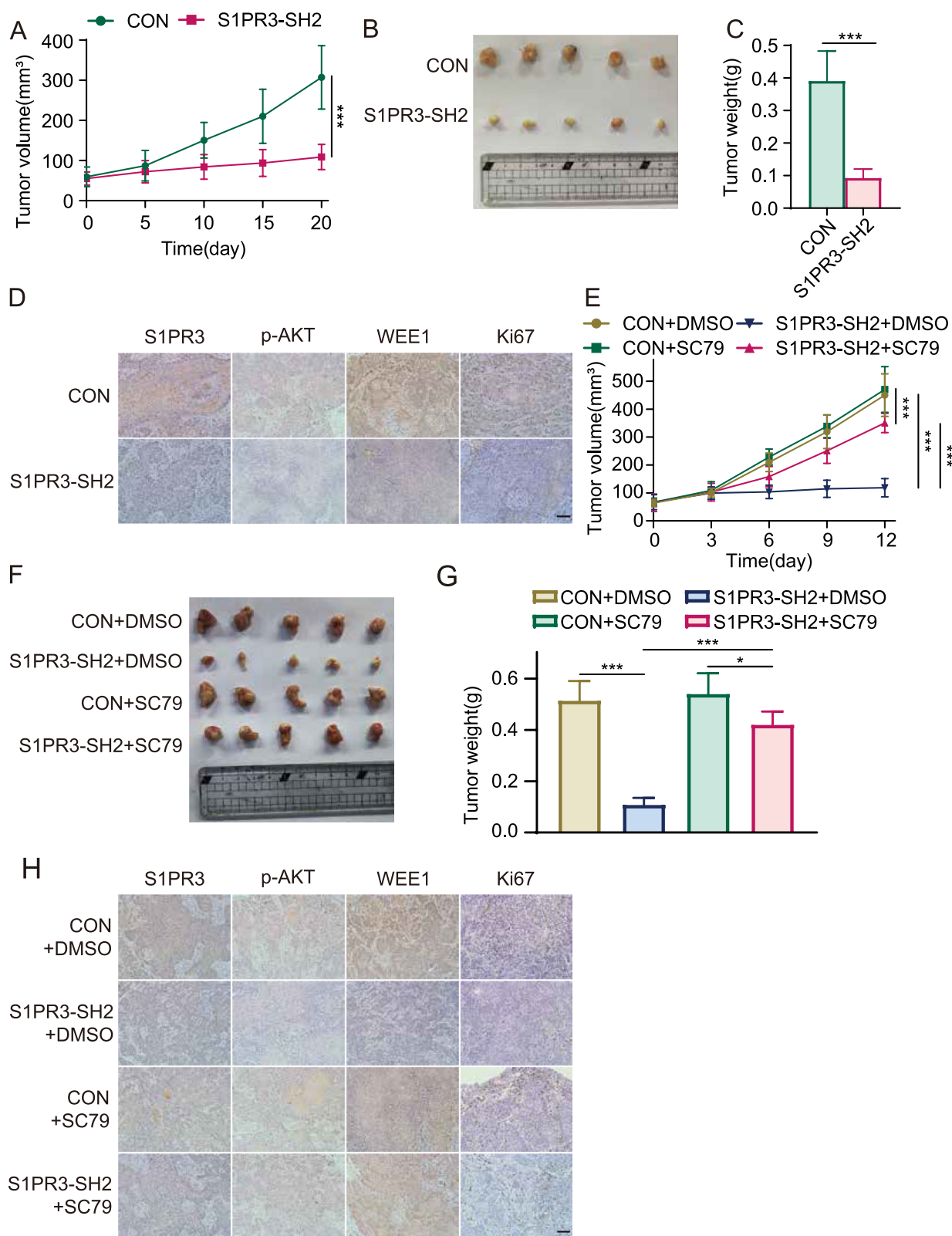


**Fig. 6** (See legend on previous page.)

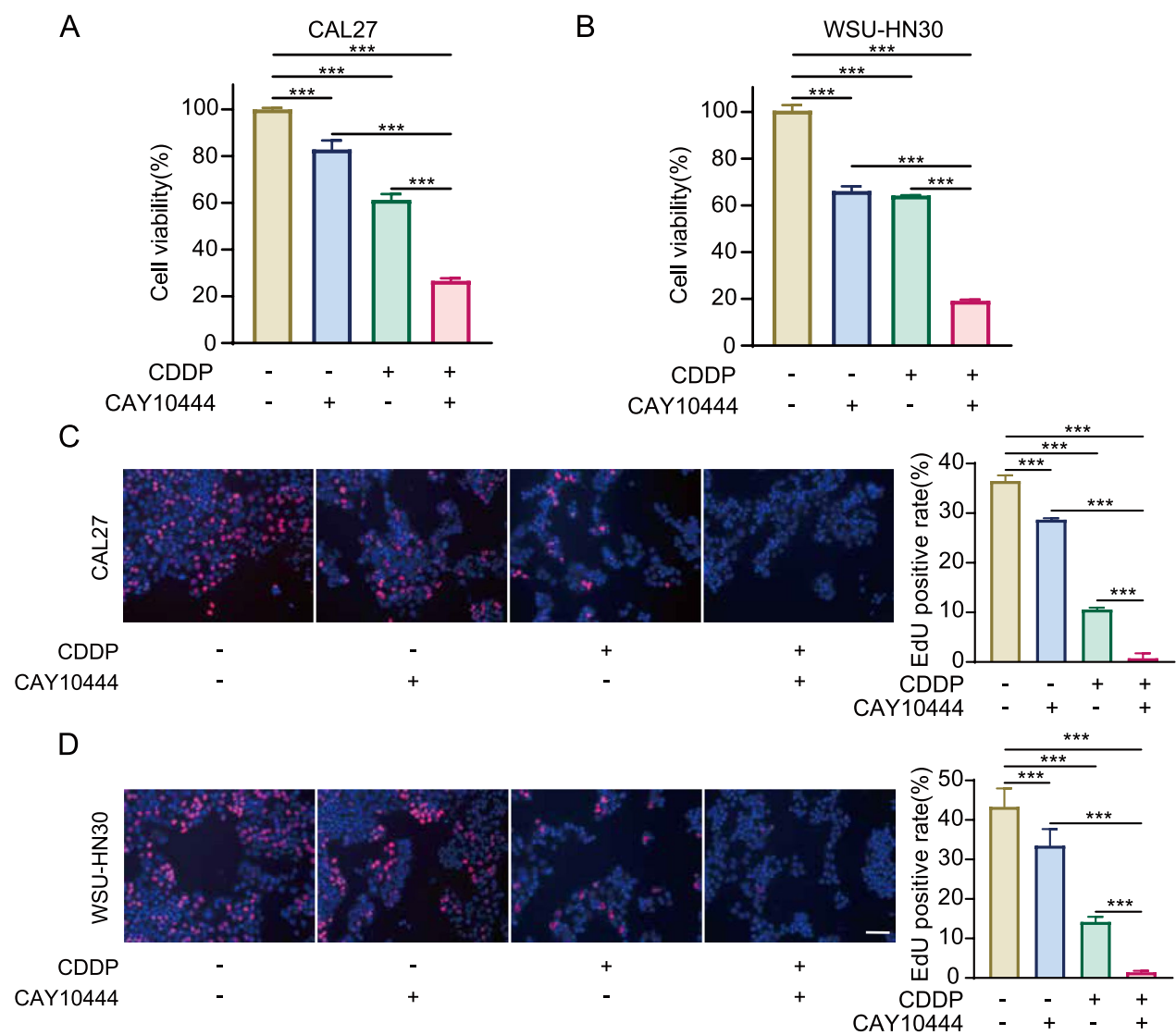


**Fig. 7** S1PR3 antagonist combined with cisplatin suppressed OSCC cells growth. **A, B** CCK8 assays were performed on CAL27 and WSU-HN30 cells subjected to CAY10444, CDDP, or the combination of CAY10444 and CDDP. **C, D** EdU incorporation assays were conducted on CAL27 and WSU-HN30 cells subjected to CAY10444, CDDP, or the combination of CAY10444 and CDDP. Data were presented as mean  $\pm$  SD, with  $n = 3$  biological replicates. \*\*\* $P < 0.001$ . Scale bar, 100  $\mu$ m



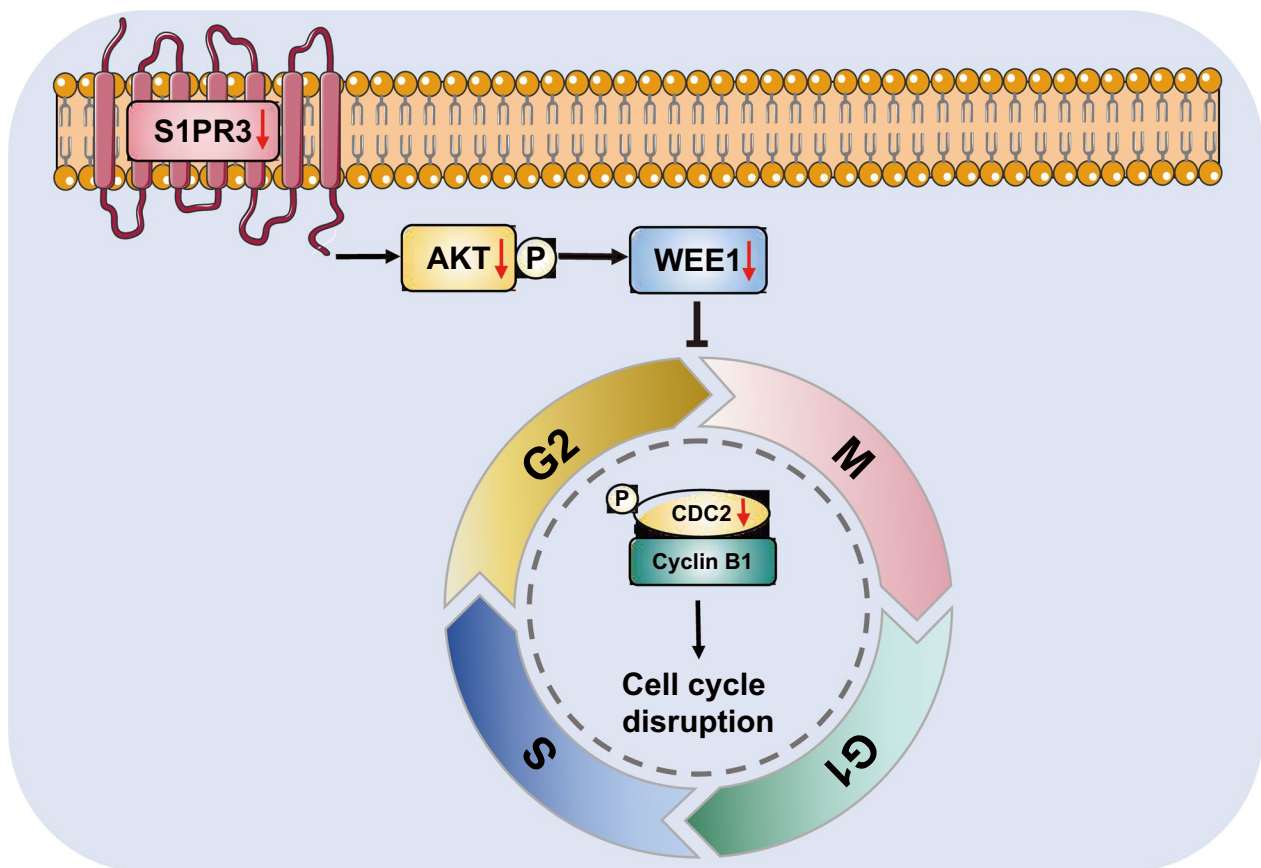


**Fig. 8** Diagram illustrating the S1PR3-mediated G2/M checkpoint failure

## Supplementary Information

The online version contains supplementary material available at <https://doi.org/10.1186/s12967-025-06582-4>.

Additional file1

Additional file 2

## Acknowledgements

The authors express gratitude to the Shanghai Key Laboratory of Stomatology for their generous provision of HaCat and HNSCC cell lines. We acknowledge the excellent technical support supplied by the Department of Oral Pathology, Ninth People's Hospital, Shanghai Jiao Tong University School of Medicine. We appreciate the linguistic assistance supplied by TopEdit ([www.topedit.com](http://www.topedit.com)) during the preparation of this manuscript.

## Author contributions

Xinxia Zhou: Project administration; methodology; validation; formal analysis; data curation; writing – original draft; Jinghao Liu: Data curation; visualization; Xu Chen: Data curation; methodology; Xinyu Zhou: Resources; methodology; Beihui Xu: Methodology; formal analysis. Guifang Gan: Writing – review and editing; conceptualization; project administration; methodology; resources. Fuxiang Chen: Writing – review and editing; funding acquisition; supervision; conceptualization; resources.

## Funding

This work was supported by the National Natural Science Foundation of China (No. 81870762, 82203551), the National Key Research and Development Program (No. 2023YFB3210305), the Fundamental Research Program Funding of the Ninth People's Hospital, Shanghai Jiao Tong University School of Medicine (No. JYJC202227), the Fundamental Research Funds for the Central Universities (No. YG2022QN065), the Shanghai Municipal Commission of Health and Family Planning (20244Y0193) and the Shanghai Jiao Tong University School of Medicine Yunxi project.

## Data availability

All data generated or analyzed during this study are included in this published article and its supplementary information files.

## Declarations

### Ethical approval

Human subjects: This study involving human subjects was conducted in accordance with the Declaration of Helsinki and approved by the Ethics Committee of Shanghai Ninth People's Hospital (SH9H-2021-T428-2). Written informed consent was obtained from all participants prior to their inclusion in the study. Animal studies: The animal experiments were approved by the Institutional Animal Care and Use Committee of Shanghai Ninth People's Hospital (SH9H-2024-A2-1) and performed in compliance with the guidelines for the care and use of laboratory animals, minimizing animal suffering throughout the experimental procedures.

**Consent for publication**

All authors agree to submit the research article for publication.

**Competing interest**

All authors declare that they have no competing interests.

**Author details**

<sup>1</sup>Department of Clinical Immunology, Shanghai Ninth People's Hospital, Shanghai Jiao Tong University School of Medicine, Shanghai 200011, China. <sup>2</sup>College of Health Science and Technology, Shanghai Jiao Tong University School of Medicine, Shanghai 200025, China. <sup>3</sup>Department of Oral and Maxillofacial-Head and Neck Oncology, College of Stomatology, Ninth People's Hospital, Shanghai Jiao Tong University School of Medicine, Shanghai 200025, China.

Received: 16 February 2025 Accepted: 7 May 2025

Published online: 23 May 2025

**References**

- Johnson DE, Burtneis B, Leemans CR, Lui VVY, Bauman JE, Grandis JR. Head and neck squamous cell carcinoma. *Nat Rev Dis Primers*. 2020;6:92.
- Chamoli A, Gosavi AS, Shirwadkar UP, Wangdale KV, Behera SK, Kurrey NK, et al. Overview of oral cavity squamous cell carcinoma: Risk factors, mechanisms, and diagnostics. *Oral Oncol*. 2021;121: 105451.
- Sung H, Ferlay J, Siegel RL, Laversanne M, Soerjomataram I, Jemal A, et al. Global Cancer Statistics 2020: GLOBOCAN Estimates of Incidence and Mortality Worldwide for 36 Cancers in 185 Countries. *CA Cancer J Clin*. 2021;71:209–49.
- Chi AC, Day TA, Neville BW. Oral cavity and oropharyngeal squamous cell carcinoma—an update. *CA Cancer J Clin*. 2015;65:401–21.
- Rezazadeh F, Andisheh-Tadib A, Malek Mansouri Z, Khademi B, Bayat P, Sedarat H, et al. Evaluation of recurrence, mortality and treatment complications of oral squamous cell carcinoma in public health centers in Shiraz during 2010 to 2020. *BMC Oral Health*. 2023;23:341.
- Abdolahinia ED, Ahmadian S, Bohlouli S, Gharehbagh FJ, Jahandizi NG, Vahed SZ, et al. Effect of curcumin on the head and neck squamous cell carcinoma cell line HN5. *Curr Mol Pharmacol*. 2023;16:374–80.
- de Medeiros MC, The S, Bellile E, Russo N, Schmitz L, Danella E, et al. Salivary microbiome changes distinguish response to chemoradiotherapy in patients with oral cancer. *Microbiome*. 2023;11:268.
- Chun J, Kihara Y, Jonnalagadda D, Blaho VA. Fingolimod: lessons learned and new opportunities for treating multiple sclerosis and other disorders. *Annu Rev Pharmacol Toxicol*. 2019;59:149–70.
- Wang P, Yuan Y, Lin W, Zhong H, Xu K, Qi X. Roles of sphingosine-1-phosphate signaling in cancer. *Cancer Cell Int*. 2019;19:295.
- Li Q, Li Y, Lei C, Tan Y, Yi G. Sphingosine-1-phosphate receptor 3 signaling. *Clin Chim Acta*. 2021;519:32–9.
- Ogretmen B. Sphingolipid metabolism in cancer signalling and therapy. *Nat Rev Cancer*. 2018;18:33–50.
- Guo Y, Ahn M-J, Chan A, Wang C-H, Kang J-H, Kim S-B, et al. Afatinib versus methotrexate as second-line treatment in Asian patients with recurrent or metastatic squamous cell carcinoma of the head and neck progressing on or after platinum-based therapy (LUX-Head & Neck 3): an open-label, randomised phase III trial. *Ann Oncol*. 2019;30:1831–9.
- Luserna G, di Rorà A, Cerchione C, Martinelli G, Simonetti G. A WEE1 family business: regulation of mitosis, cancer progression, and therapeutic target. *J Hematol Oncol*. 2020;13:126.
- Zhang Z, Richmond A, Yan C. Immunomodulatory properties of PI3K/AKT/mTOR and MAPK/MEK/ERK inhibition augment response to immune checkpoint blockade in melanoma and triple-negative breast cancer. *Int J Mol Sci*. 2022;23:7353.
- Mortazavi M, Moosavi F, Martini M, Giovannetti E, Firuzi O. Prospects of targeting PI3K/AKT/mTOR pathway in pancreatic cancer. *Crit Rev Oncol Hematol*. 2022;176: 103749.
- Ediriweera MK, Tennekoon KH, Samarakoon SR. Role of the PI3K/AKT/mTOR signaling pathway in ovarian cancer: Biological and therapeutic significance. *Semin Cancer Biol*. 2019;59:147–60.
- Hua H, Zhang H, Chen J, Wang J, Liu J, Jiang Y. Targeting Akt in cancer for precision therapy. *J Hematol Oncol*. 2021;14:128.
- Nunnery SE, Mayer IA. Targeting the PI3K/AKT/mTOR pathway in hormone-positive breast cancer. *Drugs*. 2020;80:1685–97.
- Riquelme I, Pérez-Moreno P, Mora-Lagos B, Ili C, Brebi P, Roa JC. Long non-coding RNAs (lncRNAs) as regulators of the PI3K/AKT/mTOR pathway in gastric carcinoma. *Int J Mol Sci*. 2023;24:6294.
- Xiao S, Peng K, Li C, Long Y, Yu Q. The role of sphingosine-1-phosphate in autophagy and related disorders. *Cell Death Discov*. 2023;9:380.
- Dasari S, Tchounwou PB. Cisplatin in cancer therapy: molecular mechanisms of action. *Eur J Pharmacol*. 2014;740:364–78.
- Jiang W, Chen L, Li R, Li J, Dou S, Ye L, et al. Postoperative radiotherapy with docetaxel versus cisplatin for high-risk oral squamous cell carcinoma: a randomized phase II trial with exploratory analysis of ITGB1 as a potential predictive biomarker. *BMC Med*. 2024;22:314.
- Anu B, Namitha NN, Harikumar KB. S1PR1 signaling in cancer: a current perspective. *Adv Protein Chem Struct Biol*. 2021;125:259–74.
- Sarkar J, Aoki H, Wu R, Aoki M, Hylemon P, Zhou H, et al. Conjugated bile acids accelerate progression of pancreatic cancer metastasis via S1PR2 signaling in cholestasis. *Ann Surg Oncol*. 2023;30:1630–41.
- Petti L, Rizzo G, Rubbino F, Elangovan S, Colombo P, Restelli S, et al. Unveiling role of sphingosine-1-phosphate receptor 2 as a brake of epithelial stem cell proliferation and a tumor suppressor in colorectal cancer. *J Exp Clin Cancer Res*. 2020;39:253.
- Yamashita H, Kitayama J, Shida D, Yamaguchi H, Mori K, Osada M, et al. Sphingosine 1-phosphate receptor expression profile in human gastric cancer cells: differential regulation on the migration and proliferation. *J Surg Res*. 2006;130:80–7.
- Shen Y, Zhao S, Wang S, Pan X, Zhang Y, Xu J, et al. S1P/S1PR3 axis promotes aerobic glycolysis by YAP/c-MYC/PGAM1 axis in osteosarcoma. *EBioMedicine*. 2019;40:210–23.
- Zhao J, Liu J, Lee J-F, Zhang W, Kandouz M, VanHecke GC, et al. TGF- $\beta$ /SMAD3 pathway stimulates sphingosine-1 phosphate receptor 3 expression: implication of sphingosine-1 phosphate receptor 3 in lung adenocarcinoma progression. *J Biol Chem*. 2016;291:27343–53.
- Wang W, Hind T, Lam BWS, Herr DR. Sphingosine 1-phosphate signaling induces SNAI2 expression to promote cell invasion in breast cancer cells. *FASEB J*. 2019;33:7180–91.
- Ohotski J, Long JS, Orange C, Elsberger B, Mallon E, Doughty J, et al. Expression of sphingosine 1-phosphate receptor 4 and sphingosine kinase 1 is associated with outcome in oestrogen receptor-negative breast cancer. *Br J Cancer*. 2012;106:1453–9.
- Zhang X, Cai A, Gao Y, Zhang Y, Duan X, Men K. Treatment of melanoma by nano-conjugate-delivered Wee1 siRNA. *Mol Pharmaceutics*. 2021;18:3387–400.
- Fallah Y, Demas DM, Jin L, He W, Shajahan-Haq AN. Targeting WEE1 inhibits growth of breast cancer cells that are resistant to endocrine therapy and CDK4/6 inhibitors. *Front Oncol*. 2021;11: 681530.
- Widyananda MH, Pratama SK, Samoedra RS, Sari FN, Kharisma VD, Ansori ANM, et al. Molecular docking study of sea urchin (*Arbacia lixula*) peptides as multi-target inhibitor for non-small cell lung cancer (NSCLC) associated proteins. *J Pharm Pharmacogn Res*. 2021;9:484–96.
- Scappaticcio L, Ansori ANM, Trimboli P. Editorial: Cancer-related hypercalcemia and potential treatments. *Front Endocrinol (Lausanne)*. 2023;14:1281731.
- Widyananda MH, Pratama SK, Ansori ANM, Antonius Y, Kharisma VD, Muradlo AAA, et al. Quercetin as an anticancer candidate for glioblastoma multiforme by targeting AKT1, MMP9, ABCB1, and VEGFA: an in silico study. *Karbala Int J Modern Sci*. 2023;9(3):10.
- Cooper JS, Pajak TF, Forastiere AA, Jacobs J, Campbell BH, Saxman SB, et al. Postoperative concurrent radiotherapy and chemotherapy for high-risk squamous-cell carcinoma of the head and neck. *N Engl J Med*. 2004;350:1937–44.
- Kovács AF. Response to intraarterial induction chemotherapy: a prognostic parameter in oral and oropharyngeal cancer. *Head Neck*. 2006;28:678–88.
- Liu L-Z, Zhou X-D, Qian G, Shi X, Fang J, Jiang B-H. AKT1 amplification regulates cisplatin resistance in human lung cancer cells through the mammalian target of rapamycin/p70S6K1 pathway. *Cancer Res*. 2007;67:6325–32.
- Liu Z, Qiu H, Letchmunan S, Deveci M, Abualigah L. Multi-view evidential c-means clustering with view-weight and feature-weight learning. *Fuzzy Sets Syst*. 2025;498: 109135.

40. Maiti B, Biswas S, Ezugwu AE-S, Bera UK, Alzahrani AI, Alblehai F, et al. Enhanced crayfish optimization algorithm with differential evolution's mutation and crossover strategies for global optimization and engineering applications. *Artif Intell Rev.* 2025;58:69.
41. Biswas S, Singh G, Maiti B, Ezugwu AE-S, Saleem K, Smerat A, et al. Integrating differential evolution into gazelle optimization for advanced global optimization and engineering applications. *Comput Methods Appl Mech Eng.* 2025;434: 117588.
42. Rateb R, Hadi AA, Tamanampudi VM, Abualigah L, Ezugwu AE, Alzahrani AI, et al. An optimal workflow scheduling in IoT-fog-cloud system for minimizing time and energy. *Sci Rep.* 2025;15:3607.
43. Chung W-P, Huang W-L, Liao W-A, Hung C-H, Chiang C-W, Cheung CHA, et al. FTY720 in resistant human epidermal growth factor receptor 2-positive breast cancer. *Sci Rep.* 2022;12:241.
44. Xing Y, Wang ZH, Ma DH, Han Y. FTY720 enhances chemosensitivity of colon cancer cells to doxorubicin and etoposide via the modulation of P-glycoprotein and multidrug resistance protein 1. *J Dig Dis.* 2014;15:246–59.

## Publisher's Note

Springer Nature remains neutral with regard to jurisdictional claims in published maps and institutional affiliations.